ISSN: 2834-4928

Research Article

Journal of Electrical Electronics Engineering

The Fundamental Nuclear Plasma Fusion Equation

Wim Vegt*

Department of Physics, Eindhoven University of Technology, The Netherlands

*Corresponding Author
Wim Vegt, Department of Physics, Eindhoven University of Technology, The Netherlands.

Submitted: 2025, Oct 14; **Accepted**: 2025, Nov 17; **Published**: 2025, Nov 25

Citation: Vegt, W. (2025). The Fundamental Nuclear Plasma Fusion Equation. *J Electrical Electron Eng, 4*(6), 01-24.

Abstract

Nuclear fusion represents the border area (nuclear plasma) between the material world (infusion of Deuterium) and the energy world (microwave heating). Existing theories to describe these material-energy interactions are far from the required necessary theoretical physics to realize stable nuclear fusion processes inside confinements like the Tokamak. The only possibility to describe these complex interaction processes correctly is to develop a new theory in physics which describes the electro-magnetic gravitational force density interactions (expressed in N/m³) (equation 8) with the mechanical force density interactions (expressed in N/m³) being presented by the Navier-Stokes equation for compressible nuclear plasmas [41].

The new theory, describing electro-magnetic-gravitational-acceleration force density interactions (expressed in N/m3), has been discussed at astronomical levels: Gravitational RedShift, Black Holes and Dark Matter and at sub-atomic levels: The absorption and emission of light at sub-atomic levels in concentric spheres by an atom at discrete energy levels. Evidence will be demonstrated about the correctness of this new electro-dynamic theory which represents the only theory which connects electro-dynamics in a correct way with plasma-dynamics. In general, the gravitational (acceleration) force densities, originating from rotation and linear accelerations, are being ignored but with nuclear fusion processes these gravitational (acceleration) forces become fundamental and are necessary to develop a stable nuclear fusion process.

Differently than in General Relativity, the electro-magnetic-gravitational-acceleration force density interactions (expressed in N/m3) fundamentally has been based on the divergence of the sum of the "Stress Energy Tensor" and the introduced "Gravitational-Acceleration" Tensor [33-35].

The theory describes "Gravitational-Acceleration-Electromagnetic" Interaction resulting in a mathematical Tensor presentation for BLACK HOLEs. (Gravitational Electromagnetic Confinements) The "Electromagnetic Energy Gradient" creates a second order effect "Lorentz Transformation" which results in the Gravitational Field of BLACK HOLEs which determines the interaction force density between the confinement of Light (BLACK HOLE's) and the "Gravitational-Acceleration" Field [1].

Einstein approached the interaction between gravity and light by the introduction of the "Einstein Gravitational Constant" in the 4-dimensional Energy-Stress Tensor

$\kappa \mathrm{T}_{\mu\nu}$ (1).

In this alternative approach related to General Relativity, the interaction between gravity and light has been presented by the sum of the Electromagnetic Tensor $\mathrm{T}_{\mu\nu}$ and the "Gravitational-Acceleration" Tensor $\mathrm{J}_{\mu\nu}$ (2) .

The new theory describes the impact of "CURL" within the gravitational fields around Black Holes and the impact on Gravitational Lensing. Gravitational "CURL" (Equation 6) is an effect which cannot be explained and calculated by General Relativity [36-38].

The new approach presents mathematical solutions for the BLACK HOLEs (Gravitational Electromagnetic Interaction) introduced in 1955 by Jonh Archibald Wheeler in the publication in Physical Review Letters in 1955 [1]. The mathematical solutions for BLACK HOLEs are fundamental solutions for the relativistic quantum mechanical Dirac equation (Quantum Physics) in Tensor presentation (41).

Assuming a constant speed of light "c" and Planck's constant ħ within the BLACK HOLE, the radius "R" of the BLACK HOLE with the energy of a proton, is about 1% of the radius of the hydrogen atom (14).

The New Theory has been tested in an experiment with 2 Galileo Satellites and a Ground Station by measuring the Gravitational RedShift in an by the Ground Station emitted stable MASER frequency [2]. The difference between the calculation for Gravitational RedShift, within the Gravitational Field of the Earth, in "General Relativity" and the "New Theory" is smaller than 10^{-16} (12) and (13).

In all "General Redshift Experiments" "General Relativity" and the New Electrodynamic-Gravitational-Acceleration" Theory predict a Gravitational RedShift with a difference smaller than 15 digits beyond the decimal point which is beyond the accuracy of modern "Gravitational Redshift" observations. Both values are always within the measured Gravitational RedShift in all observations being published since the first observation of the gravitational redshift in the spectral lines from the White Dwarf which was the measurement of the shift of the star Sirius B, the white dwarf companion to the star Sirius, by W.S. Adams in 1925 at Mt. Wilson Observatory.

Theories which unify Quantum Physics and General Relativity [32], like "String Theory", predict the non-constancy of natural constants. Accurate observations of the NASA Messenger observe in time a value for the gravitational constant "G" which constrains until (|G| /G to be $< 4 \times 10^{-14}$ per year) . One of the characteristics of the New Theory is the "Constant Value" in time for the Gravitational Constant "G" in unifying General Relativity and Quantum Physics [7-11].

Keywords: Quantum Physics, General Relativity, Gravitational RedShift, Black Holes, Dark Matter, Nuclear Fusion, Nuclear Plasmas

1. An Alternative Approach in Gravity and Acceleration

Einstein approached the interaction between gravity and light by the introduction of the "Einstein Gravitational Constant" in the 4-dimensional Energy-Stress Tensor.

$$\mathrm{G}_{\mu\nu} + \Lambda\, \mathrm{g}_{\mu\nu} = \kappa\, \mathrm{T}_{\mu\nu} \tag{1}$$

In which $\mathrm{G}_{\mu\nu}$ equals the Einstein Tensor, $\mathrm{g}_{\mu\nu}$ equals the Metric Tensor, $\mathrm{T}_{\mu\nu}$ equals the Stress-Energy tensor, Λ equals the cosmological constant and κ equals the Einstein gravitational constant.

An alternative approach to Einstein's expression with the tensor $\kappa \mathrm{T}_{\mu\nu}$, describing the curvature of the Space-Time continuum, is the sum of the Electromagnetic Tensor $\mathrm{T}_{\mu\nu}$ and the "Gravitational-Acceleration" Tensor $\mathrm{J}_{\mu\nu}$.

$$\kappa\, \mathrm{T}_{\mu\nu} \Leftrightarrow \mathrm{T}_{\mu\nu} + \mathrm{J}_{\mu\nu} \tag{2}$$

The 4-dimensional divergence of the sum of the Electromagnetic Stress-Energy tensor and the Gravitational Tensor expresses the 4-dimensional Force-Density vector (expressed in [N/m³] in the 3 spatial coordinates) as the result of Electro- Magnetic-Gravitational interaction.

$$f^{\mu} = \partial_{\nu} \left(\mathrm{T}^{\mu\nu} + \mathrm{J}^{\mu\nu} \right) \tag{3}$$

In vector notation the 4-dimensional Force-Density vector can be written as:

$$\overline{f}^{4} = \begin{pmatrix} f_4 \\ f_3 \\ f_2 \\ f_1 \end{pmatrix} = \Box \bullet \left(\overline{\overline{\mathrm{T}}} + \overline{\overline{\mathrm{J}}} \right) \tag{4}$$

The fundamental boundary condition for this alternative approach to gravity is the requirement that the Force 4 vector equals zero in the 4 dimensions, expressing a universal 4-dimensional equilibrium:

$$\overline{f}^4 = \begin{pmatrix} f_4 \\ f_3 \\ f_2 \\ f_1 \end{pmatrix} = \Box \bullet \left(\overline{\overline{\mathrm{T}}} + \overline{\overline{\mathrm{J}}} \right) = \overline{0}^4 \qquad (5)$$

The 3 spatial components of the Force-Density vector, as a result of Electro-Magnetic-Gravitational interaction can be written as:

$$\overline{f} = -\frac{1}{c^2}\frac{\partial\,(\overline{\mathrm{E}} \times \overline{\mathrm{H}})}{\partial t} + \varepsilon_0\, \overline{\mathrm{E}}\,(\nabla\,.\,\overline{\mathrm{E}}) - \varepsilon_0\, \overline{\mathrm{E}} \times (\nabla \times \overline{\mathrm{E}}) +$$

$$+\mu_0\, \overline{\mathrm{H}}\,(\nabla\,.\,\overline{\mathrm{H}}) - \mu_0\, \overline{\mathrm{H}} \times (\nabla \times \overline{\mathrm{H}}) + \gamma_0\, \overline{\mathrm{g}}\,(\nabla\,.\,\overline{\mathrm{g}}) - \gamma_0\, \overline{\mathrm{g}} \times (\nabla \times \overline{\mathrm{g}}) = \overline{0} \quad [\mathrm{N/m^3}]$$

in which:

$\varepsilon_0\,(\nabla\,.\,\overline{\mathrm{E}}) = \rho_{\mathrm{E}}$ Electric Charge Density $[\mathrm{C/m^3}]$

$\mu_0\,(\nabla\,.\,\overline{\mathrm{H}}) = \rho_M$ Magnetic Flux Density $[\mathrm{Vs/m^3}]$ or $[\mathrm{Wb/m^3}]$ (6)

$\gamma_0\,(\nabla\,.\,\overline{\mathrm{g}}) = \rho_M$ Mass Density (Electromagnetic) $[\mathrm{kg/m^3}]$

Electric Energy Density: $\mathrm{w_E} = \frac{1}{2}\varepsilon_0\,\mathrm{E}^2$

Magnetic Energy Density: $\mathrm{w_M} = \frac{1}{2}\mu_0\,\mathrm{H}^2$

Gravitational Energy Density: $\mathrm{w_G} = \frac{1}{2}\gamma_0\,\mathrm{g}^2$

$\overline{\mathrm{g}} \triangleq$ acceleration (gravitational or mechanical/dynamical)

In which E represents the electric field intensity expressed in [V/m], H represents the magnetic field intensity expressed in [A/m] and g represents the gravitational acceleration expressed in [m/s^2]. The permittivity indicated as ε_0 the permeability indicated as μ_0 and the gravitational permeability of vacuum as γ_0.

For curl-free gravitational fields equation (6) can be written as:

$$\overline{f} = -\frac{1}{c^2}\frac{\partial\,(\overline{\mathrm{E}} \times \overline{\mathrm{H}})}{\partial t} + \varepsilon_0\, \overline{\mathrm{E}}\,(\nabla\,.\,\overline{\mathrm{E}}) - \varepsilon_0\, \overline{\mathrm{E}} \times (\nabla \times \overline{\mathrm{E}}) +$$

$$+\mu_0\, \overline{\mathrm{H}}\,(\nabla\,.\,\overline{\mathrm{H}}) - \mu_0\, \overline{\mathrm{H}} \times (\nabla \times \overline{\mathrm{H}}) + \overline{\mathrm{g}}\,\rho_M = \overline{0} \quad [\mathrm{N/m^3}] \qquad (7)$$

Substituting Einstein's W = m c^2 in (7) results in "Electro-Magnetic-Gravitational Equilibrium Field Equation" (8):

$$\overline{f} = -\frac{1}{c^2}\frac{\partial\,(\overline{\mathrm{E}} \times \overline{\mathrm{H}})}{\partial t} + \varepsilon_0\, \overline{\mathrm{E}}\,(\nabla\,.\,\overline{\mathrm{E}}) - \varepsilon_0\, \overline{\mathrm{E}} \times (\nabla \times \overline{\mathrm{E}}) + \qquad (8)$$

$$+\mu_0\, \overline{\mathrm{H}}\,(\nabla\,.\,\overline{\mathrm{H}}) - \mu_0\, \overline{\mathrm{H}} \times (\nabla \times \overline{\mathrm{H}}) + \frac{1}{2\,\mathrm{c}^2}\overline{\mathrm{g}}\left(\varepsilon\,\mathrm{E}^2 + \mu\,\mathrm{H}^2\right) = \overline{0} \quad [\mathrm{N/m^3}]$$

The theory describes "Electromagnetic-Gravitational Interaction", "Magnetic Gravitational Interaction" and "Electric-Gravitational Interaction". In this new theory particles do not interact with fields. The interaction between an electric charged particle and an electric field is not the interaction between a particle and a field but it is the interaction between the electric field of the particle interacting with the other electric field. Every interaction is an interaction between fields. Electric Fields interact with Electric Fields, Magnetic Fields interact with Magnetic Fields and Gravitational Fields interact with Gravitational Fields.

2. "Gravitational RedShift/ BlueShift in "Light (EMR)" due to "Electromagnetic Gravitational Interaction"

To test the New Theory, the Gravitational-Redshift experiment: "Test of the Gravitational Redshift with Galileo Satellites in an Eccentric Orbit" by S. Hermann et all, has been chosen [2]. In this experiment a stable "MASER" frequency from a ground station has been emitted to 2 Galileo Satellites, measuring the frequency difference between the Ground Station and the Satellites. The frequency shift has been caused by the gravitational field of the Earth and 2 satellites has been chosen to compensate for the eccentricity of the Galileo Orbit.

Assuming a gravitational field g[z] depending on the radial direction in cartesian coordinates between the ground station and the satellites:

$$\overline{\mathrm{g[z]}} = \left\{0,0,\ \frac{G\ \mathrm{M}_{Earth}}{4\ \pi\ \mathrm{z}^2}\right\} \tag{9}$$

In which G (G = 6.67428 10^{-11} Nm^2 / kg^2) equals the Gravitational constant, MEarth the mass of the earth and r the radial distance from the centre of the earth. The mathematical solution of equation (8) for plane electromagnetic waves (expressed in cartesian {x,y,z} coordinates) related to the Electric Field Intensity equals [5,6].

$$\overline{\mathrm{E}} = \begin{pmatrix} \mathrm{E_x} \\ \mathrm{E_y} \\ \mathrm{E_z} \end{pmatrix} = \begin{pmatrix} e^{-\frac{\mathrm{G\,M}_{Eearth}\ \varepsilon_0\ \mu_0}{8\ \pi\ \mathrm{z}}}\ \mathrm{h}\left[\ \omega_0\ e^{-\frac{\mathrm{G\,M}_{Earth}\ \varepsilon_0\ \mu_0}{4\ \pi\ \mathrm{z}}}\left(\mathrm{t} - \sqrt{\varepsilon\ \mu}\ \mathrm{z}\right)\right] \\ 0 \\ 0 \end{pmatrix} \tag{10}$$

And the mathematical solution of (8) for the Magnetic Field Intensity equals:

$$\overline{\mathrm{H}} = \begin{pmatrix} \mathrm{H_x} \\ \mathrm{H_y} \\ \mathrm{H_z} \end{pmatrix} = \begin{pmatrix} 0 \\ \frac{1}{\sqrt{\varepsilon_0\ \mu_0}}\ e^{-\frac{\mathrm{G\,M}_{Earth}\ \varepsilon_0\ \mu_0}{8\ \pi\ \mathrm{z}}}\ \mathrm{h}\left[\ \omega_0\ e^{-\frac{\mathrm{G\,M}_{Earth}\ \varepsilon_0\ \mu_0}{4\ \pi\ \mathrm{z}}}\left(\mathrm{t} - \sqrt{\varepsilon\ \mu}\ \mathrm{z}\right)\right] \\ 0 \end{pmatrix} \tag{11}$$

In which ω_0 equals the original frequency of the MASER radiation propagating in the direction of the gravitational field g[z] of the Earth in the z-direction. The exponential term demonstrates the Gravitational Redshift when the MASER radiation propagates in the direction of the Gravitational Field of the earth. The propagation speed of the Electromagnetic Radiation remains constant (the speed of light). But the amplitude of the field intensity and the frequency of the field intensity diminishes exponentially.

Calculations in Mathematica demonstrate a difference between the calculation with General Relativity and the calculation with the New Theory [5]. Choosing for the ground station a distance to the centre of the earth z_1 = 6,378,000 [m] (Radius of the Earth) and for the average distance of the ESA satellites in a Galileo orbit z_2 = 23,222,000 [m] (distance from the ESA satellite to the centre of the Earth), calculated with Mathematica, the Gravitational RedShift according General Relativity equals:

$$\Delta\ \omega_{GR} = 0.0000000000401815497097883\ [\mathrm{s}^{-1}] \tag{12}$$

Calculated with Mathematica, the Gravitational RedShift according the New Theory, which is a solution of equation (8) equals:

$$\Delta\ \omega_{GR} = 0.0000000000401824206173742\ [\mathrm{s}^{-1}] \tag{13}$$

Both calculated values a within the Range of the measured gravitational RedShift by the average values of both ESA satellites in the Galileo orbit

$$\Delta\,\omega_{\text{Measured}} = 0.000000000040118 \ \pm 2.2\ 10^{-15} \quad [s^{-1}] \qquad (14)$$

In [2] a factor α has been defined which presents the measured deviation α between the predicted Gravitational RedShift by General Relativity and the Measured Gravitational RedShift.

$$\alpha = \Delta\,\omega_{\text{MEASURED}} - \Delta\,\omega_{\text{GR}} = (2.2 \pm 1.6) \times 10^{-5} \qquad (15)$$

A comparable factor α can be used to determine which theory (General Relativity or the New Theory) has the nearest approach to the experimentally measured data. Highly accurate measuring experiments are required with an accuracy higher than 16 digits beyond the decimal point.

3. Black Holes

3.1 Black Holes Without Singularities with Dimensions Smaller Than the Diameter of the Hydrogen Atom

A second fundamental solution for equation (8) describes a Gravitational Electromagnetic Confinement (BLACK HOLE) within a radial gravitational field [1]. with acceleration $\underline{g}$ (in radial direction). This solution represents a Black Hole, the confinement of light due to its own gravitational field, and has no singularities. This solution for equation (8) describes Black Holes, dependent of time and radius, presenting discrete spherical energy levels, within a radial gravitational field with acceleration $\bar{g}$ (in radial direction) has been represented in (16) and (17) [14].

$$\begin{pmatrix} E_r \\ E_\theta \\ E_\varphi \end{pmatrix} = \begin{pmatrix} 0 \\ f(r)\ \mathrm{Sin}(k\,r)\ \mathrm{Sin}(\omega\,t) \\ -f(r)\ \mathrm{Cos}(k\,r)\ \mathrm{Cos}(\omega\,t) \end{pmatrix} \quad \begin{pmatrix} H_r \\ H_\theta \\ H_\varphi \end{pmatrix} = \sqrt{\frac{\varepsilon}{\mu}} \begin{pmatrix} 0 \\ -f(r)\ \mathrm{Sin}(k\,r)\ \mathrm{Cos}(\omega\,t) \\ -f(r)\ \mathrm{Cos}(k\,r)\ \mathrm{Sin}(\omega\,t) \end{pmatrix} \quad \bar{g} = \begin{pmatrix} \dfrac{G_1}{4\pi r^2} \\ 0 \\ 0 \end{pmatrix} \qquad (16)$$

$$w_{em} = \left(\frac{\mu_0}{2}\left(\bar{m} \cdot \bar{m}\right) + \frac{\varepsilon_0}{2}\left(\bar{e} \cdot \bar{e}\right) \right) =$$

$$f(r)^2 \left(\left(\mathrm{Sin}(k\,r)\ \mathrm{Sin}(\omega\,t)\right)^2 + \left(\mathrm{Cos}(k\,r)\ \mathrm{Cos}(\omega\,t)\right)^2 + \frac{\varepsilon}{\mu}\left(\mathrm{Sin}(k\,r)\ \mathrm{Cos}(\omega\,t)\right)^2 + \left(\mathrm{Cos}(k\,r)\ \mathrm{Sin}(\omega\,t)\right)^2 \right)$$

In which the radial function f(r) equals:

$$f[r] = K\ e^{-\frac{G\ M_{BH}\ \varepsilon_0\,\mu_0}{8\pi r}} \qquad (17)$$

G represents the Gravitational constant and M represents the total confined electromagnetic mass of the BLACK HOLE. Equation (16) presents a Standing (Confined) Electromagnetic Field Configuration with a phase shift of 90 degrees between the electric field and the magnetic field with the corresponding Nodes and AntiNodes [12,13]. The solution has been calculated according Newton's Shell Theorem, resulting in the fundamental concept of the "Prima Materia" [43].

Assuming a constant speed of light "c" and Planck's constant ħ within the BLACK HOLE, the radius "R" (with n = 1,2,3,4….) of the BLACK HOLE with the energy of a proton, according $W = m_{proton}\, c^2$, would be: $1.5009211 \times 10^{-10}$ [J].

$$R_{\text{GEON}} = n\,\lambda = n\left(\frac{c}{f}\right) = n\left(\frac{c}{W}\right)\hbar = 7.1865\ 10^{-26}\left(\frac{n}{W}\right) \qquad (18)$$

$$R_{GEON} = n\ 3.82\ 10^{-12}\ [m]$$

Black Holes are varying from atomic dimensions with dimensions of 10^{-27} [kg], Page 39 [33] until Black Holes with dimensions of 10^{40} [kg], Page 67 [34]. At these dimensions Black Holes turn into Dark Matter. The fundamental boundary condition for the confinement of Electromagnetic radiation (BLACK HOLEs) is that the energy flow (Poynting vector) $\overline{S} = \overline{E} \times \overline{H}$ equals zero at the surfcace of the confinement. This is possible at every "*90 degrees Phase Shift Surface*" (Sphere) between the Electric Field and the Magnetic Field.

3.1 Black Holes with a Singular Point and Large Dimensions

Figure1 represents a Black Hole with a mass of 10^{35} [kg] and a radius of about 25 [km] controlled by a different mahgematical solution for equation (8). The radius of the Black Hole equals about 25 [km] which has been controlled by a different mathematical solution (19) for equation (8).

$$f[r] = K\ e^{\left(\frac{G\, M_{BH}\ \varepsilon_0\, \mu_0}{8\,\pi\, r} - \log[r]\right)} \quad [J/m^3] \qquad (19)$$

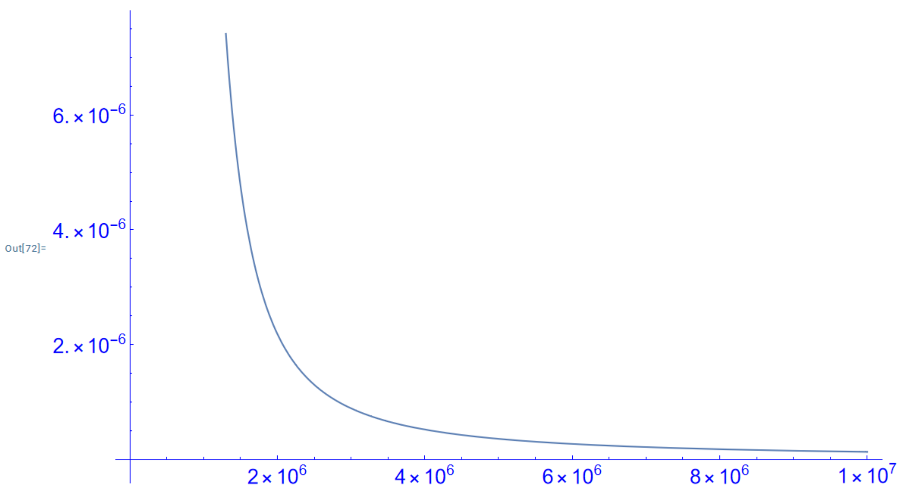

Figure 1: The Energy Density [J/ m³] as a function of the Radius R = max 10^7 [m] of the Black Hole

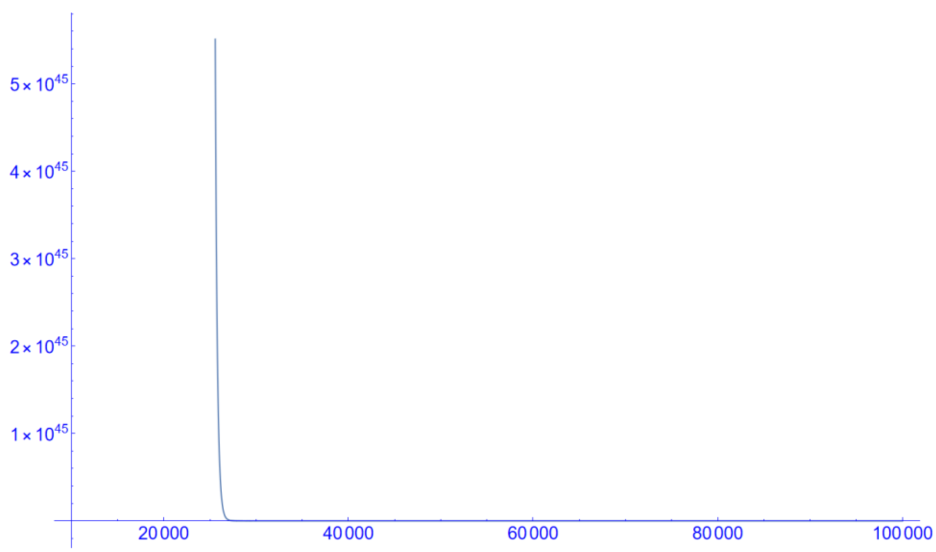

Figure 2: The Energy Density [J/ m³] as a function of the Radius R = max 10^5 [m]

Figure 1 and Figure 2 demonstrate the large effect of "Gravitational Intensity Shift" and "Gravitational RedShift" at the distance of 25 [km]. Over a distance of 10.000 [km] the intensity of the emitted light of the Black Hole with a mass of 10^{35} [kg] falls back with a factor of 10^{-51}. Also the frequency of the emitted light of the Black Hole falls back with a factor 10^{-51}. Emitted light in the visible spectrum of 10^{14} [Hz] falls back to a frequency of 10^{-37} [Hz]. These extreme low frequencies with extreme low intensities have never been measured which has result in the name "Black Hole" for the phenomenon of "Gravitational Intensity Shift" and "Gravitational RedShift" for a large mass. It follows from equation (8) and the solutions (10) and (11) that the speed of light does not change inside and around Black Hole. Only the direction of the propagation of light can change due to a gravitational field.

3.2. Dark Matter in the Universe Controlled by "Gravitational Shielding"

Figure 3 represents Dark Matter with a total mass of 10^{53} [kg] and a radius of about 10 times the size of the Milky Way Galaxy. The radius of the dark mass equals 5 10^{21} [m] which has been controlled by a different mathematical solution (20) for equation (8).

$$f[r] = K\ e^{\left(\frac{G\ M_{BH}\ \varepsilon_0\ \mu_0}{8\ \pi\ r} - \log[r]\right)} \quad [\mathrm{J} / \mathrm{m}^3] \tag{20}$$

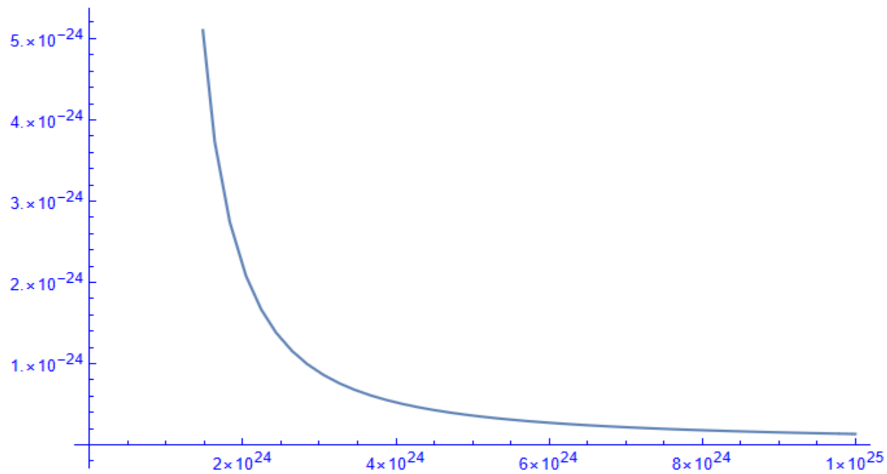

Figure 3: The Energy Density [J/ m^3] as a function of the Radius R = max 10^{25} [m] of the Dark Matter

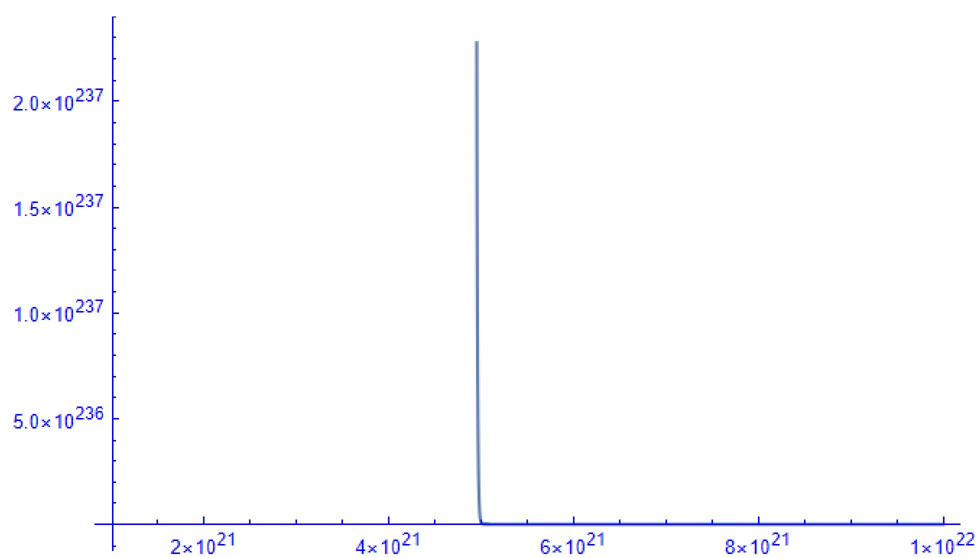

Figure 4: The Energy Density [J/ m^3] of the Dark Matter as a function of the Radius R = max 10^{22} [m]

Figures 3 and 4 serve to illustrate the profound impact of "Gravitational Intensity Shift" and "Gravitational RedShift" at a distance of 5 x 10^{21} [m], an expanse tenfold the radius of the Milky Way Galaxy. Across this vast distance, the luminosity of light emitted by the Dark Matter entity possessing a mass of 10^{53} [kg] drastically diminishes by an extraordinary factor of 10^{-261}. Correspondingly, the frequency of the light emitted from this Dark Matter entity also decreases by a striking factor of 10^{-261}. Initial light emissions within the visible spectrum around 1014 [Hz] regress to an exceptionally low frequency of 10^{-24747} [Hz]. These profoundly reduced frequencies, accompanied by drastic diminutions in intensity, have led to the designation "Dark Matter" to describe the phenomenon marked by "Gravitational Intensity Shift" and "Gravitational RedShift" evident in realms of significant mass.

Fundamentally, as inferred from equation (8) and solutions (10) and (11), the speed of light remains invariant within and surrounding the Dark Mass. The gravitational field of the Dark Mass primarily influences the directional propagation of light while preserving the constancy of the speed of light.

4. The Relationship between Black Holes and Quantum Physics

Introducing the Quantum Vector Function $\overline{\phi}$,

$$\overline{\phi} = \sqrt{\frac{\mu}{2}} \left(\overline{\mathrm{H}} + \mathrm{i}\, \frac{\overline{\mathrm{E}}}{c} \right) \tag{21}$$

Substituting (21) in (16) results in the quantum presentation for the BLACK HOLE:

$$\overline{\Phi(r,\theta,\varphi)} = \sqrt{\frac{\mu}{2}} \left(\overline{\mathrm{H}} + \mathrm{i}\, \frac{\overline{\mathrm{E}}}{c} \right) \mathrm{f(r)} \begin{pmatrix} \Phi_r \\ \Phi_\theta \\ \Phi_\varphi \end{pmatrix}$$

(22)

$$\overline{\Phi(r,\theta,\varphi)} = K \sqrt{\frac{\varepsilon}{\mu}}\, \mathrm{e}^{-\frac{G1\, \varepsilon_0\, \mu_0}{8\,\pi\,\mathrm{r}}} \begin{pmatrix} 0 & 0 & 0 \\ 0 & -\mathrm{Sin}(\mathrm{k\,r}) & \mathrm{Sin}(\mathrm{k\,r}) \\ 0 & -\mathrm{i\,Cos}(\mathrm{k\,r}) & \mathrm{i\,Cos}(\mathrm{k\,r}) \end{pmatrix} \begin{Bmatrix} 0 \\ \mathrm{Cos}\,(\omega\,\mathrm{t}) \\ \mathrm{i\,Sin}\,(\omega\,\mathrm{t}) \end{Bmatrix}$$

With "K" a constant value dependend of the mass of the BLACK HOLE. The Dot product between the unit vector and the Quantum Vector Function $\overline{\phi}$ represents the quantum mechanical probability function $\Psi[r,\mathrm{t}]$ which is a fundamental solution of the Schrödinger Wave Equation.

$$\overline{\Phi(r,\theta,\varphi)} = K \sqrt{\frac{\varepsilon}{\mu}}\, \mathrm{e}^{-\frac{G1\, \varepsilon_0\, \mu_0}{8\,\pi\,\mathrm{r}}} \begin{pmatrix} 0 & 0 & 0 \\ 0 & -\mathrm{Sin}(\mathrm{k\,r}) & \mathrm{Sin}(\mathrm{k\,r}) \\ 0 & -\mathrm{i\,Cos}(\mathrm{k\,r}) & \mathrm{i\,Cos}(\mathrm{k\,r}) \end{pmatrix} \begin{Bmatrix} 0 \\ \mathrm{Cos}\,(\omega\,\mathrm{t}) \\ \mathrm{i\,Sin}\,(\omega\,\mathrm{t}) \end{Bmatrix}$$

(23)

$$\Psi(\mathrm{r},\mathrm{t}) = \{1\ \ 1\ \ 1\} \begin{Bmatrix} 0 \\ \mathrm{Cos}\,(\omega\,\mathrm{t}) \\ \mathrm{i\,Sin}\,(\omega\,\mathrm{t}) \end{Bmatrix} K \sqrt{\frac{\varepsilon}{\mu}}\, \mathrm{e}^{-\frac{G1\, \varepsilon_0\, \mu_0}{8\,\pi\,\mathrm{r}}} = K \sqrt{\frac{\varepsilon}{\mu}}\, \mathrm{e}^{-\frac{G1\, \varepsilon_0\, \mu_0}{8\,\pi\,\mathrm{r}}}\, \mathrm{e}^{\mathrm{i}\,\omega\,\mathrm{t}}$$

The Scalar function $\Psi[r,\mathrm{t}]$ represents a fundamental solution of the Quantum Mechanical Schrödinger wave equation. [36, 37]

4.1 Black Holes with Discrete Spherical Energy Levels at Sub-Atomic dimensions

A crucial criterion for effectively confining Electromagnetic Energy entails ensuring that the Poynting vector equates to zero at the spherical surface delineating the confines. Specifically, to encapsulate this energy within a sphere, the setup necessitates a standing electromagnetic wave configuration characterized by concentric spheres. At each sphere boundary, there exists an antinodal plane for either the Electric Field (E) or Magnetic Field (B), with a radial distance separating each sphere that corresponds to half the wavelength of the taken confinement. The relationship is governed by the defined constant k = nπλ, where "n" pertains to a natural number sequence (1, 2, 3, 4, and so forth), and λ signifies the wavelength of the electromagnetic wave being considered.

4.1.1 Time and Radius Dependent Black Holes with Discrete Energy Levels. The Confinements of Electromagnetic Radiation within spherical Regions

Each concentric sphere serves as an antinodal surface for either the Electric Field (E) or the Magnetic Field (H). At these boundaries, the Poynting Vector^ is precisely zero at any given time and location within the sphere. Notably, the confinement ensures that Electromagnetic Energy remains contained within the boundaries of each sphere and transitions seamlessly to the subsequent concentric sphere. The distinctive property of these concentric spheres lies in the variance of their radii, set at one half wavelength of the electromagnetic radiation within the enclosure, reflecting discrete energy levels. It is important to note that each concentric sphere functions as an antinodal surface for either the electric or magnetic field, contributing to the structured confinement of electromagnetic energy within the system.

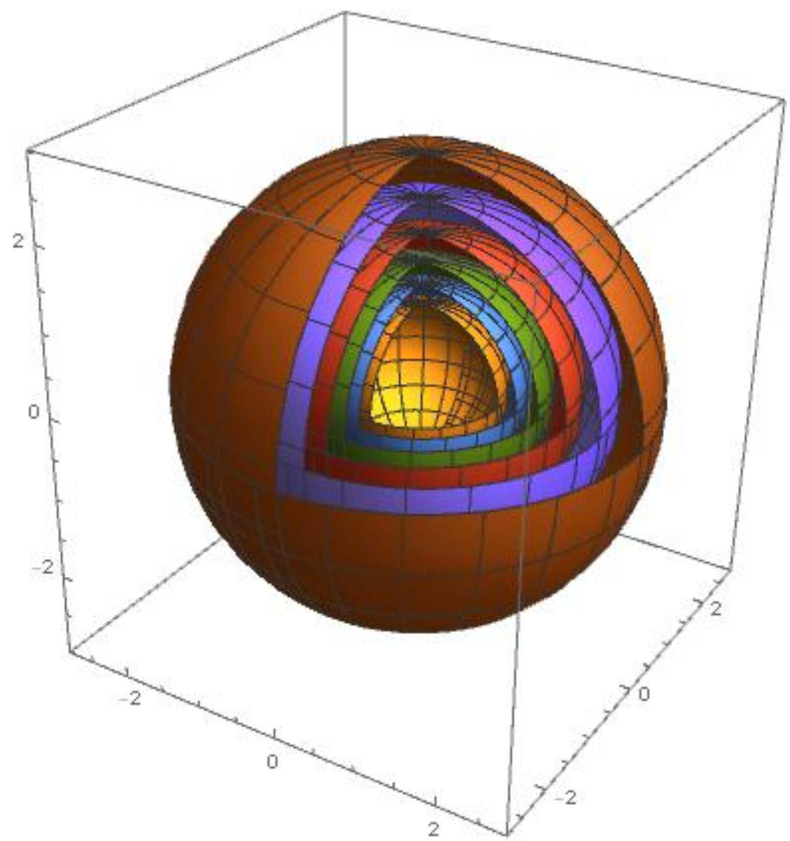

Figure 5: Nodal and Antinodal Spheres for Standing (Confined) Spherical Electromagnetic waves with a 90 degrees phase shift between the Electric field and the Magnetic field. Equation (9)

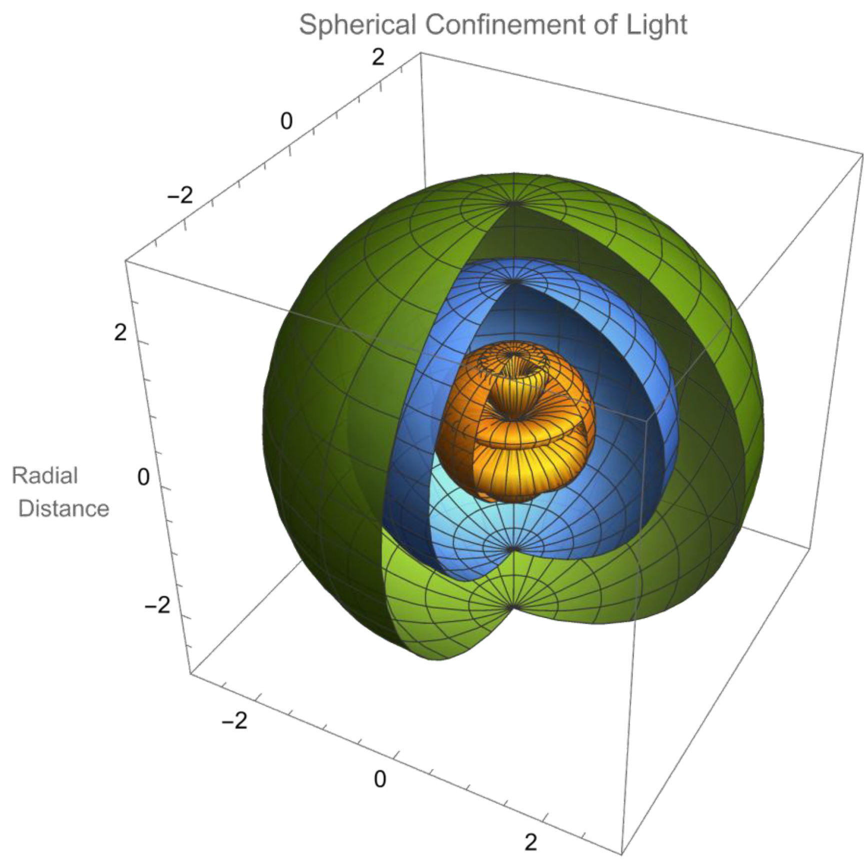

Figure 6: Nodal- and Antinodal Spheres (k = 3) for Standing (Confined) Spherical Electromagnetic waves with a 90 degrees phase shift between the Electric field and the Magnetic field. Equation (9)

Equation (24) describes a Time and Radius dependent BLACK HOLE.

$$\overline{\mathrm{E}} = \mathrm{K}\, e^{-\frac{G1\varepsilon 0 \mu 0}{8\pi r}} \begin{pmatrix} 0 \\ \mathrm{Sin}[k\, r]\ \mathrm{Sin}[\omega\, t] \\ -\ \mathrm{Cos}[k\, r]\ \mathrm{Cos}[\omega\, t] \end{pmatrix}$$

$$\overline{\mathrm{H}} = \mathrm{K}\, e^{-\frac{G1\epsilon 0 \mu 0}{8\pi r}} \sqrt{\frac{\varepsilon_0}{\mu_0}} \begin{pmatrix} 0 \\ \mathrm{Sin}[k\, r]\ \mathrm{Cos}[\omega\, t] \\ -\ \mathrm{Cos}[k\, r]\ \mathrm{Sin}[\omega\, t] \end{pmatrix} \tag{24}$$

Equation (20) represents by the function Sin[k r] (k = 1,2,3,4….) the confinement of electromagnetic radiation between two concentric spheres. K represents the amplitude of the Electric/ Magnetic Field Intensty [14].

4.1.2 Time and Polar Angle Dependent Black Holes

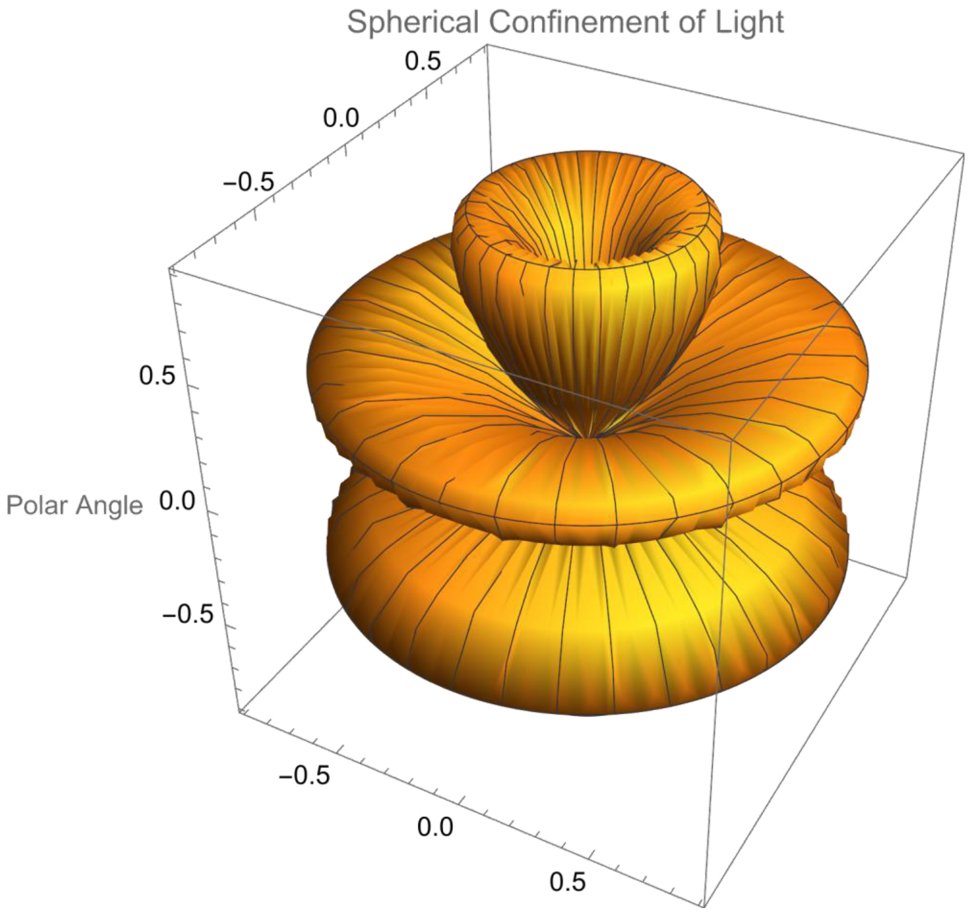

Figure 7: Nodal- and Antinodal Polar Angle Regions (m = 3) for Standing (Confined) Spherical Electromagnetic waves with a 90 degrees phase shift between the Electric field and the Magnetic field. Equation (15)

Equation (25) describes a Time and "Polar Angle" dependent BLACK HOLE

$$\overline{\mathrm{E}} = \mathrm{K}\, e^{-\frac{G1\varepsilon 0\mu 0}{8\pi r}} \begin{pmatrix} 0 \\ \mathrm{Sin}[\mathrm{m}\ \theta]\ \mathrm{Sin}[\omega\ \mathrm{t}] \\ \mathrm{Sin}[\mathrm{m}\ \theta]\ \mathrm{Cos}[\omega\ \mathrm{t}] \end{pmatrix} \qquad (25)$$

$$\overline{\mathrm{H}} = \mathrm{K}\, e^{-\frac{G1\epsilon 0\mu 0}{8\pi r}} \sqrt{\frac{\varepsilon_0}{\mu_0}} \begin{pmatrix} 0 \\ \mathrm{Sin}[\mathrm{m}\ \theta]\ \mathrm{Cos}[\omega\ \mathrm{t}] \\ -\ \mathrm{Sin}[\mathrm{m}\ \theta]\ \mathrm{Sin}[\omega\ \mathrm{t}] \end{pmatrix}$$

Equation (19) represents by the function Sin[m θ] (m = 1,2,3,4…..) the confinement of electromagnetic radiation between two Polar Angular Regions [15].

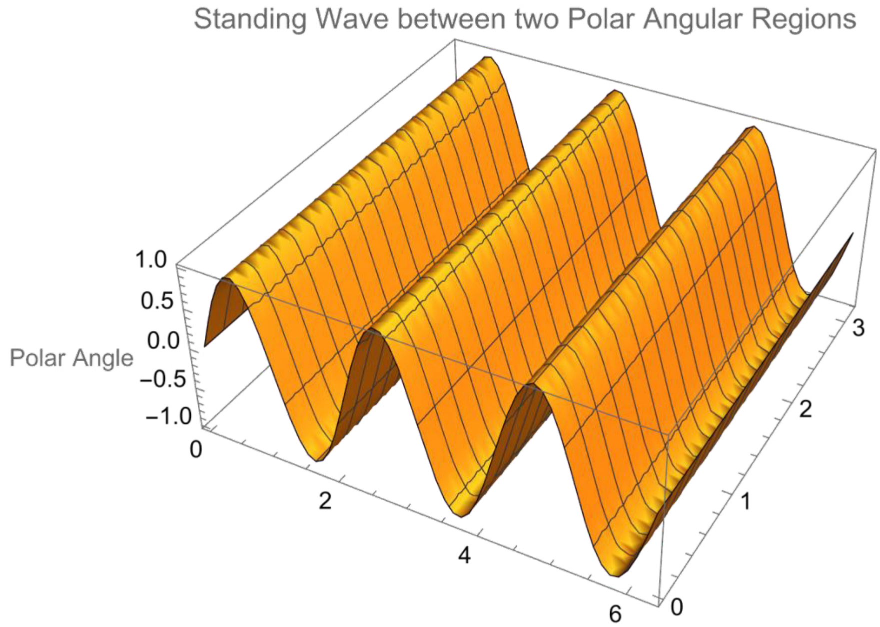

Figure 8: Nodal- and Antinodal Polar Angle Regions (m = 3) for Standing (Confined) Electromagnetic waves with a 90 degrees phase shift between the Electric field and the Magnetic field. Equation (15)

4.1.3 Time and Azimuthal Angular Dependent Black Holes

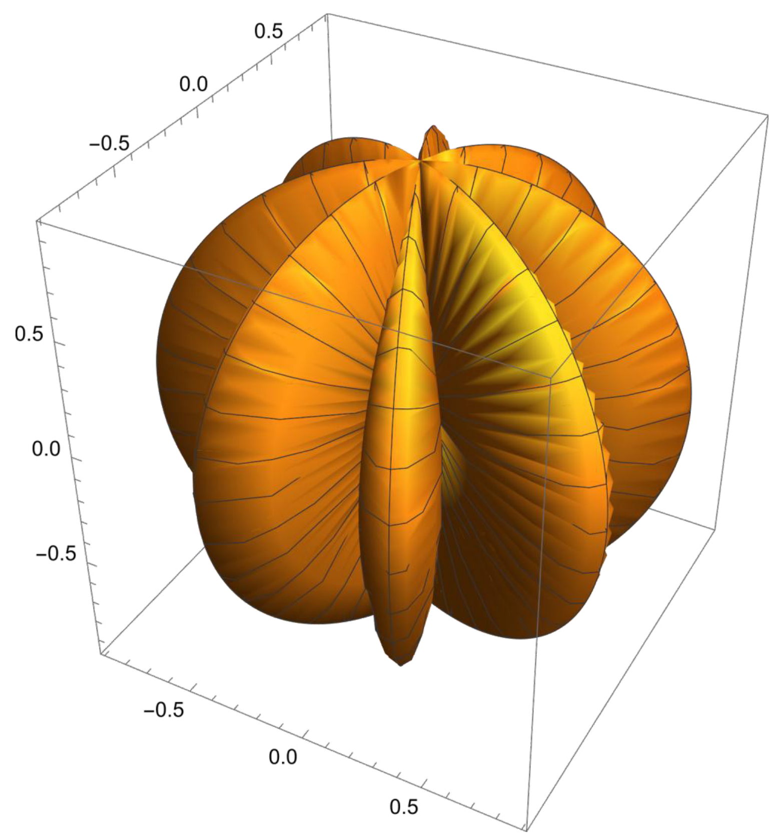

Figure 9: Nodal- and Antinodal Azimuthal Angular Regions (n = 3) for Standing (Confined) Electromagnetic waves with a 90 degrees phase shift between the Electric field and the Magnetic field. Equation (16)

Equation (26) describes a Time and “Polar Angle” dependent BLACK HOLE

$$\overline{\mathrm{E}} = \mathrm{K}\, e^{-\frac{G1\varepsilon 0\mu 0}{8\pi r}} \begin{pmatrix} 0 \\ \mathrm{Cos}[n\ \varphi]\ \mathrm{Sin}[\omega\ t] \\ \mathrm{Cos}[n\ \varphi]\ \mathrm{Cos}[\omega\ t] \end{pmatrix}$$

$$\overline{\mathrm{H}} = \mathrm{K}\, e^{-\frac{G1\epsilon 0\mu 0}{8\pi r}} \sqrt{\frac{\varepsilon_0}{\mu_0}} \begin{pmatrix} 0 \\ \mathrm{Cos}[n\ \varphi]\ \mathrm{Cos}[\omega\ t] \\ -\ \mathrm{Cos}[n\ \varphi]\ \mathrm{Sin}[\omega\ t] \end{pmatrix} \tag{26}$$

Equation (26) represents by the function Sin[n] φ (n = 1,2,3,4…..) the confinement of electromagnetic radiation between two Azimuthal Angular Regions [16].

4.1.4 Time, Polar- and Azimuthal Angular dependent Black Holes

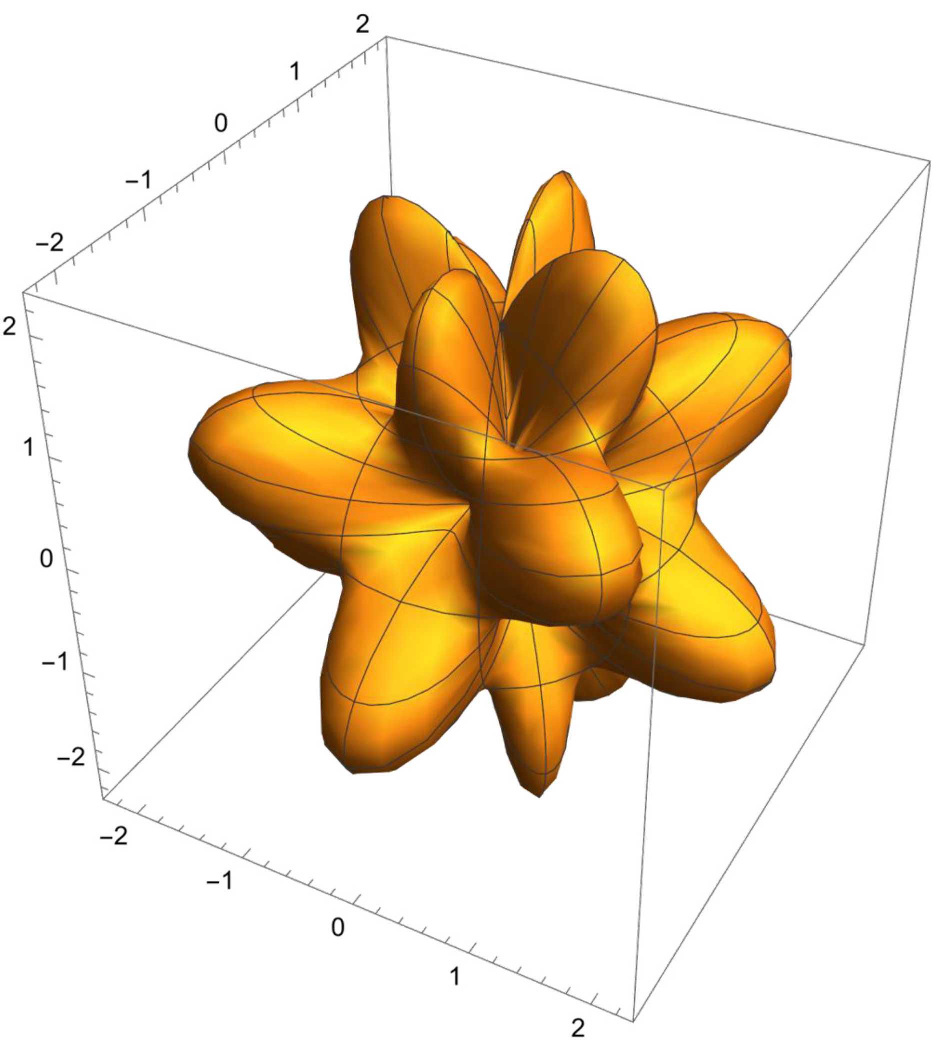

Figure 10: Nodal- and Antinodal Polar Angular and Azimuthal Angular Regions (n = 4 and m = 4) for Standing (Confined) Electromagnetic waves with a 90 degrees phase shift between the Electric field and the Magnetic field. Equation (17)

Equation (27) describes a Time “Azimuthal Angle” and “Polar Angle” dependent BLACK HOLE

$$\overline{\mathrm{E}} = \mathrm{K}\, e^{-\frac{G1\varepsilon 0\mu 0}{8\pi r}} \begin{pmatrix} 0 \\ \mathrm{Cos}[n\ \varphi]\ \mathrm{Sin}[m\ \theta]\ \mathrm{Sin}[\omega\ t] \\ \mathrm{Cos}[n\ \varphi]\ \mathrm{Sin}[m\ \theta]\ \mathrm{Cos}[\omega\ t] \end{pmatrix}$$

$$\overline{\mathrm{H}} = \mathrm{K}\, e^{-\frac{G1c0\mu 0}{8\pi r}} \sqrt{\frac{\varepsilon_0}{\mu_0}} \begin{pmatrix} 0 \\ -\mathrm{Cos}[n\ \varphi]\ \mathrm{Sin}[m\ \theta]\ \mathrm{Cos}[\omega\ t] \\ \mathrm{Cos}[n\ \varphi]\ \mathrm{Sin}[m\ \theta]\ \mathrm{Sin}[\omega\ t] \end{pmatrix} \tag{27}$$

Equation (27) represents by the function Cos[n φ] (n = 1,2,3,4…..) and Sin[m φ] (m = 1,2,3,4…..) the confinement of electromagnetic radiation between two Azimuthal Angular Regions and two Polar Angulars Regions [17].

4.1.5 Spherical Confinement of Light beween two Concentric Spheres within Black Holess

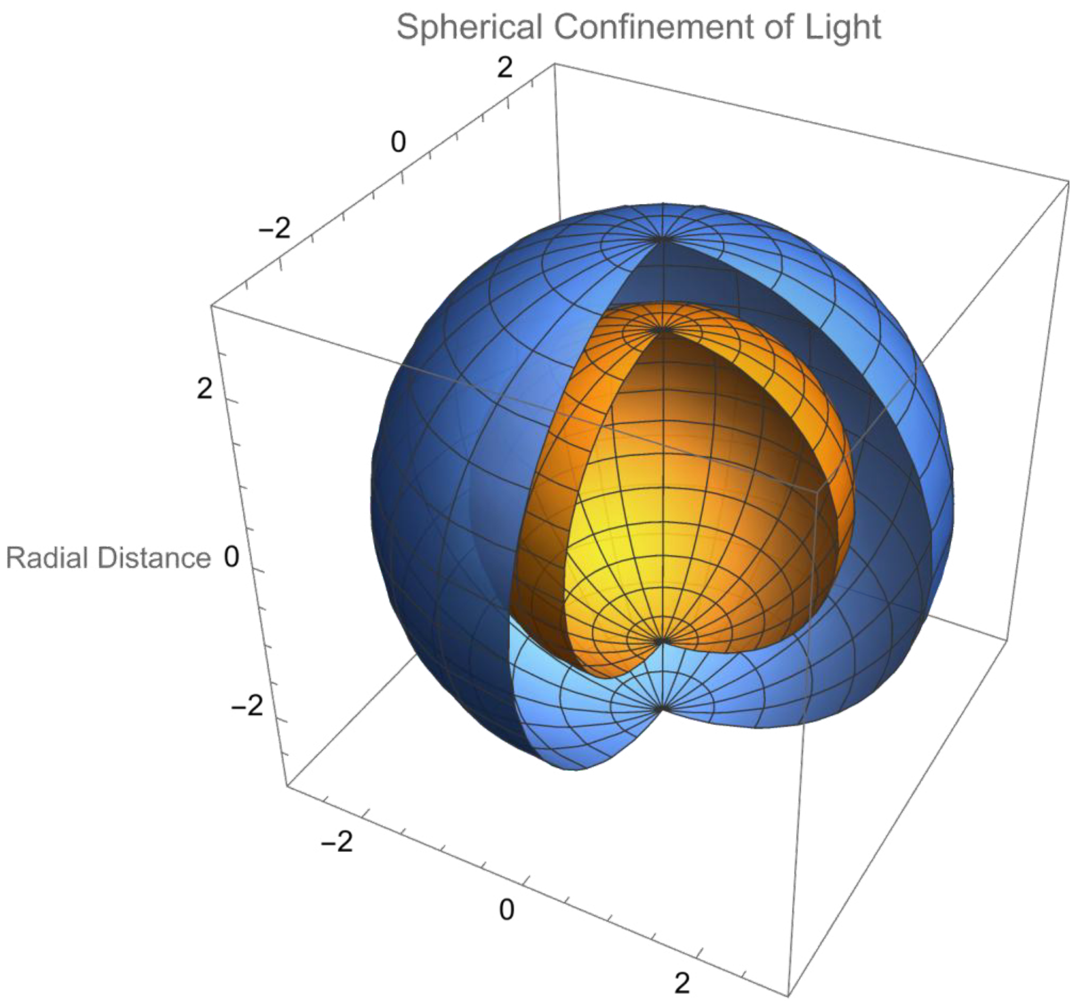

Figure 11: Nodal- and Antinodal Regions for Standing (Confined) Electromagnetic waves with a 90 degrees phase shift between the Electric field and the Magnetic field. Equation (14)

Equation (18) elucidates the mirrored propagation of the Confined Electromagnetic Energy within the BLACK HOLE, encompassed between two successive concentric spheres [21-25]. Notably, the speed of light, contingent upon the variable "r," experiences alterations in direction concurrent with variations in the frequency of the confined light, representing the Electromagnetic Radiation.

In a transformative manner, a BLACK HOLE has the capacity to bifurcate into two distinctive entities, each characterized by a different radius. This metamorphosis manifests as the original BLACK HOLE regresses into a lower energy state, akin to an atom transitioning to a lower energy level. Concurrently, the emergence of the new BLACK HOLE symbolizes the contrast in energy levels, mirroring the dynamics of an atom cascading to a lower energy state within its structure.

$$\bar{E} = K\, e^{-\frac{G1\varepsilon 0\mu 0}{8\pi r}}\, f\left[t - \frac{\sqrt{\varepsilon_0\ \mu_0}\ \mathrm{Cos}[2\,k\,r]}{2\,k}\right] \begin{pmatrix} 0 \\ \mathrm{Sin}[k\,r]\ \mathrm{Sin}[\omega\,t] \\ -\mathrm{Cos}[k\,r]\ \mathrm{Cos}[\omega\,t] \end{pmatrix}$$

(28)

$$\bar{H} = K\, e^{-\frac{G1\epsilon 0\mu 0}{8\pi r}}\, f\left[t - \frac{\sqrt{\varepsilon_0\ \mu_0}\ \mathrm{Cos}[2\,k\,r]}{2\,k}\right] \sqrt{\frac{\varepsilon_0}{\mu_0}} \begin{pmatrix} 0 \\ -\mathrm{Sin}[k\,r]\ \mathrm{Cos}[\omega\,t] \\ -\mathrm{Cos}[k\,r]\ \mathrm{Sin}[\omega\,t] \end{pmatrix}$$

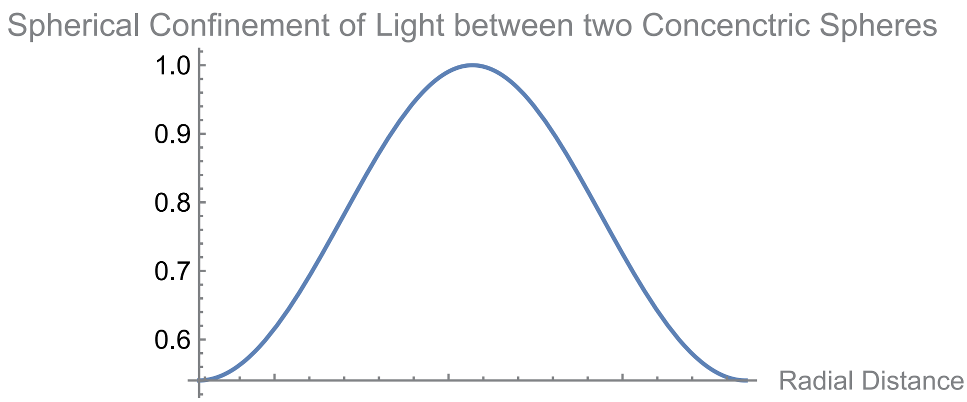

Figure 12: Nodal- and Antinodal Regions for Standing (Confined) Electromagnetic within two concentric spheres. Equation (18)

5. Universal Equilibrium in the "Concept of Quantum Mechanical Probability" in "The New Theory"

The 4-dimensional notation for the divergence of the Stress-Energy Tensor (25) expresses in the 4th dimension (time dimension) the law of Conservation of Energy". For an Electromagnetic Field the law for conservation of Energy has been expressed as:

$$\bar{f}^4 = \begin{pmatrix} f_4 \\ f_3 \\ f_2 \\ f_1 \end{pmatrix} = \Box \bullet \bar{\bar{T}} = \begin{pmatrix} \nabla \cdot \bar{S} + \frac{\partial w}{\partial t} \\ f_3 \\ f_2 \\ f_1 \end{pmatrix} = \bar{0}^4 \qquad (29)$$

From the derivation of the equation governing the "Conservation of Electromagnetic Energy" (38.1), we can extract the crux of the matter: the derivation of the "Fundamental Equation for Confined Electromagnetic Interaction" within "The New Theory." This fundamental equation aligns closely with the Relativistic Quantum Mechanical "Dirac" equation and the Schrödinger wave equation, particularly at velocities significantly lower in magnitude relative to the speed of light,[25-32].

In essence, this "Fundamental Equation for Confined Electromagnetic Interaction" within "The Proposed Theory" essentially embodies a relativistic iteration of the Quantum Mechanical Schrödinger wave equation, effectively mirroring the attributes of the Quantum Mechanical Dirac Equation within the context of this modified theoretical framework.

5.1 Confined Electromagnetic Energy within a 4-Dimensional Equilibrium

The inception of the concept of quantum mechanical probability waves emerged during the renowned 1927 5th Solvay Conference, marking a significant milestone in the realm of quantum mechanics. Amidst this era, a confluence of circumstances uniquely converged to birth the profound idea of "Material Waves" derived from solutions of Schrödinger's wave equation, characterized by their intrinsically complex nature—partly real and partly imaginary. These waves, known as "Quantum Mechanical Probability Waves," delineate the likelihood of a physical entity, typically an elementary particle, manifesting within a given system.

The notion of complex probability waves is intrinsically linked to the notion of confined standing waves. A distinguishing feature of any standing acoustical wave is the inherent phase shift over 90 degrees between Velocity and Pressure (analogous to Electric Field and Magnetic Field in Quantum Electrodynamics). This fundamental principle extends to standing electromagnetic waves as well, highlighting a consistent pattern where the Velocity (Pressure) and the Electric Field (Magnetic Field) exhibit a 90-degree phase separation in these confined wave structures.

For that reason every confined (standing) Electromagnetic wave can be described by a complex sum vector $\bar{\phi}$ of the Electric Field Vector $\bar{\mathrm{E}}$ and the Magnetic Field Vector $\bar{\mathbf{B}}$ ($\bar{\mathrm{E}}$ has 90 degrees phase shift compared to $\bar{\mathbf{B}}$).

The vector functions $\bar{\phi}$ and the complex conjugated vector function $\bar{\phi}^*$ will be written as:

$$\bar{\phi} = \frac{1}{\sqrt{2\,\mu}} \left(\bar{\mathrm{B}} + \mathrm{i}\, \frac{\bar{\mathrm{E}}}{c} \right) \tag{30}$$

$\bar{\mathbf{B}}$ equals the magnetic induction, $\bar{\mathrm{E}}$ the electric field intensity ($\bar{\mathrm{E}}$ has + 90 degrees phase shift compared to $\bar{\mathbf{B}}$) and c the speed of light.

The complex conjugated vector function $\bar{\phi}^*$ equals:

$$\overline{\phi^*} = \frac{1}{\sqrt{2\,\mu}} \left(\bar{\mathrm{B}} - \mathrm{i}\, \frac{\bar{\mathrm{E}}}{c} \right) \tag{31}$$

The dot product equals the electromagnetic energy density w:

$$\bar{\phi} \,.\, \overline{\phi^*} = \frac{1}{2\,\mu} \left(\bar{\mathrm{B}} + \mathrm{i} \frac{\bar{\mathrm{E}}}{c} \right) . \left(\bar{\mathrm{B}} - \mathrm{i} \frac{\bar{\mathrm{E}}}{c} \right) = \frac{1}{2}\, \mu\, \mathrm{H}^2 + \frac{1}{2}\, \varepsilon\, \mathrm{E}^2 = \mathrm{w} \tag{32}$$

Using Einstein's equation $W = m\,c^2$, the dot product equals the electromagnetic mass density w:

$$\bar{\phi} \,.\, \overline{\phi^*} \frac{1}{c^2} = \frac{\varepsilon}{2} \left(\bar{\mathrm{B}} + \mathrm{i}\, \frac{\bar{\mathrm{E}}}{c} \right) . \left(\bar{\mathrm{B}} - \mathrm{i}\, \frac{\bar{\mathrm{E}}}{c} \right) = \frac{1}{2} \varepsilon\, \mu^2 \mathrm{H}^2 + \frac{1}{2} \varepsilon^2 \mathrm{E}^2 = \rho \ [\mathrm{kg/m^3}] \tag{33}$$

The cross product is proportional to the Poynting vector (Ref. 3, page 202, equation 15).

$$\bar{\phi} \times \overline{\phi^*} = \frac{1}{2\,\mu} \left(\bar{\mathrm{B}} + \mathrm{i}\, \frac{\bar{\mathrm{E}}}{c} \right) \times \left(\bar{\mathrm{B}} - \mathrm{i}\, \frac{\bar{\mathrm{E}}}{c} \right) = \mathrm{i} \sqrt{\varepsilon\, \mu}\ \ \bar{\mathrm{E}} \times \bar{\mathrm{H}} = \mathrm{i} \sqrt{\varepsilon\, \mu}\ \bar{\mathrm{S}} \tag{34}$$

This article unveils a groundbreaking "Gravitational-Electromagnetic Equation," delineating configurations of Electromagnetic Fields that serve as both the solutions for the Scalar Quantum Mechanical "Schrödinger Wave Equation" and more precisely, the mathematical solutions aligning with the Tensor representation of the "Relativistic Quantum Mechanical Dirac Equation" (41).

The 4-dimensional divergence computed from the amalgamated Electromagnetic Stress-Energy tensor signifies a pivotal advancement. It elucidates the manifestation of a 4-dimensional Force-Density vector, expressed in units of [N/m^3] across the three spatial coordinates. This vector elegantly encapsulates the intricate interplay of Electro-Magnetic-Gravitational interactions, unveiling a deeper understanding of the forces at play within these multifaceted electromagnetic fields.

$$f^{\mu} = \partial_{\nu} \mathrm{T}^{\mu\nu} = 0 \tag{35}$$

In vector notation the 4-dimensional Force-Density vector can be written as:

$$\overline{f}^{4} = \begin{pmatrix} f_4 \\ f_3 \\ f_2 \\ f_1 \end{pmatrix} = \Box \bullet \overline{\overline{\mathrm{T}}} = 0 \tag{36}$$

In this alternative gravitational framework, a pivotal boundary condition mandates that the Force 4-vector attains a state of equilibrium across the four dimensions, constituting a universal 4-dimensional balance:

Expressing the spatial components of the Force-Density vector arising from Electromagnetic-Gravitational interaction yields:

Upon substituting the pertinent electromagnetic attributes for the electric field intensity denoted as "E" and the magnetic field intensity designated as "H" into equation (36), the outcome entails the 4-dimensional formulation of the Electromagnetic-Gravitational Fields Equation (37). This representation encapsulates the intricate dynamics of the electromagnetic and gravitational interplay within this novel gravitational paradigm.

Energy-Time Domain

$$\left(\mathrm{f}_4\right) \quad \Leftrightarrow \quad \nabla \cdot (\overline{\mathrm{E}} \times \overline{\mathrm{H}}) + \frac{1}{2} \frac{\partial\left(\varepsilon_0 \left(\overline{\mathrm{E}} \cdot \overline{\mathrm{E}}\right) + \mu_0 \left(\overline{\mathrm{H}} \cdot \overline{\mathrm{H}}\right)\right)}{\partial t} = 0$$

3-Dimensional Space Domain

(37)

$$\begin{pmatrix} \mathrm{f}_3 \\ \mathrm{f}_2 \\ \mathrm{f}_1 \end{pmatrix} \quad \Leftrightarrow \quad - \frac{1}{c^2} \frac{\partial (\overline{\mathrm{E}} \times \overline{\mathrm{H}})}{\partial t} + \varepsilon_0 \overline{\mathrm{E}} (\nabla \cdot \overline{\mathrm{E}}) - \varepsilon_0 \overline{\mathrm{E}} \times (\nabla \times \overline{\mathrm{E}})$$

$$+ \mu_0 \overline{\mathrm{H}} (\nabla \cdot \overline{\mathrm{H}}) - \mu_0 \overline{\mathrm{H}} \times (\nabla \times \overline{\mathrm{H}}) = \overline{0}$$

In which f_1 , f_2 , f_3, represent the force densities in the 3 spatial dimensions and f4 represent the force density (energy flow) in the time dimension (4^{th} dimension). Equation (37) can be written as:

Energy-Time Domain

Conservation of Energy

B-7

$$\left(\mathrm{f}_4\right) \qquad \nabla \cdot \overline{\mathrm{S}} + \frac{\partial \mathrm{w}}{\partial t} = 0 \tag{38.1}$$

3-Dimensional Space Domain

(38)

$$\begin{pmatrix} f_3 \\ f_2 \\ f_1 \end{pmatrix} \quad \underbrace{- \frac{1}{c^2} \frac{\partial (\bar{E} \times \bar{H})}{\partial t}}_{\text{B-1}} + \underbrace{\varepsilon_0 \bar{E} (\nabla . \bar{E})}_{\text{B-2}} - \underbrace{\varepsilon_0 \bar{E} \times (\nabla \times \bar{E})}_{\text{B-3}} + \underbrace{+ \mu_0 \bar{H} (\nabla . \bar{H})}_{\text{B-4}} - \underbrace{\mu_0 \bar{H} \times (\nabla \times \bar{H})}_{\text{B-5}} = \bar{0} \qquad (38.2)$$

The 4th term in equation (38.1) can be written in the terms of the Poynting vector "S" and the energy density "w" representing the electromagnetic law for the conservation of energy (Newton's second law of motion).

5.3 The 4-Dimensional Relativistic Dirac Equation

Substituting (32) and (34) in Equation (38.1) results in The 4-Dimensional Tensor presentation for the relativistic quantum mechanical Dirac Equation (39):

$$(x_4) \qquad \nabla . (\bar{\phi} \times \overline{\phi^*}) + \frac{i}{c} \frac{\partial \bar{\phi} . \bar{\phi}^*}{\partial t} = 0$$

$$\begin{pmatrix} x_3 \\ x_2 \\ x_1 \end{pmatrix} \quad \frac{i}{c} \frac{\partial (\bar{\phi} \times \overline{\phi^*})}{\partial t} - \left(\bar{\phi} \times (\nabla \times \overline{\phi^*}) + \overline{\phi^*} \times (\nabla \times \bar{\phi}) \right) + \left(\bar{\phi} \; (\nabla . \overline{\phi^*}) + \overline{\phi^*} \; (\nabla . \bar{\phi}) \right) = 0 \qquad (39)$$

To transform the electromagnetic vector wave function $\bar{\phi}$ into a scalar (spinor or onedimensional matrix representation), the Pauli spin matrices σ and the following matrices (Ref. 3 page 213, equation 99) are introduced:

$$\bar{\alpha} = \begin{bmatrix} 0 & \sigma \\ \sigma & 0 \end{bmatrix} \quad \text{and} \quad \bar{\beta} = \begin{bmatrix} \delta_{ab} & 0 \\ 0 & -\delta_{ab} \end{bmatrix} \qquad (40)$$

The Equations (6), (32) and (34) can be written in tensor presentation as the 4-Dimensional Relativistic Quantum Mechanical Dirac Equation: [3] (Equation 102, page 213)

$$(x_4) \qquad \left(\frac{i\,m\,c}{h} \bar{\beta} + \bar{\alpha} . \nabla \right) \psi = - \frac{1}{c} \frac{\partial \psi}{\partial t} \qquad (41.1)$$

(41)

$$\begin{pmatrix} x_3 \\ x_2 \\ x_1 \end{pmatrix} \quad - \frac{1}{c^2} \frac{\partial (\bar{E} \times \bar{H})}{\partial t} + \varepsilon_0 \bar{E} (\nabla . \bar{E}) - \varepsilon_0 \bar{E} \times (\nabla \times \bar{E}) + + \mu_0 \bar{H} (\nabla . \bar{H}) - \mu_0 \bar{H} \times (\nabla \times \bar{H}) + \gamma_0 \bar{g} (\nabla . \bar{g}) - \gamma_0 \bar{g} \times (\nabla \times \bar{g}) = \bar{0} \qquad (41.2)$$

6. The Fundamental Nuclear Plasma-Fusion Stability Equation

In the realm of thermonuclear-heated plasma, a complex interplay of "mechanical electromagnetic-gravitational interactions" transpires [42]. These interactions manifest between the ionized nuclear plasma, which engenders electromagnetic fields within the plasma itself, and the powerful external field stemming from the heating microwave radiation.

Central to this intricate system is the fundamental boundary condition governing the interactions within the plasma. This condition dictates that at any given moment, in any spatial direction, the total force densities f measured in [N/m³] must consistently sum up to zero across the entire volume encompassed within the construction of the Tokamak. This equilibrium is paramount for sustaining stability and harmonious functioning within the Tokamak structure amidst the dynamic interplay of forces.

$$\bar{f} = \rho \left(\frac{\partial \bar{v}}{\partial t} + \bar{v} \cdot \nabla \bar{v} \right) + \nabla p - \nabla \cdot \left(\zeta \left(\nabla \bar{v} + \left(\nabla \bar{v} \right)^T \right) - \frac{2}{3} \zeta \left(\nabla \cdot \bar{v} \right) \bar{\bar{I}} \right)$$

$$- \varepsilon_0 \overline{E_E} (\nabla . \overline{E_P}) + \mu_0 \overline{H_E} \times (\nabla \times \overline{H_P}) + \frac{1}{c^2} \frac{\partial (\overline{E_E} \times \overline{H_E})}{\partial t} + \frac{1}{c^2} \frac{\partial (\overline{E_P} \times \overline{H_P})}{\partial t} + \varepsilon_0 \overline{E_E} \times (\nabla \times \overline{E_P})$$

$$- \mu_0 \overline{H_E} (\nabla . \overline{H_P}) - \bar{g} \left(\frac{1}{2 c^2} \left(\varepsilon E_E{}^2 + \mu H_E{}^2 \right) \right) - \gamma_0 \bar{g} (\nabla . \bar{g}) + \gamma_0 \bar{g} \times (\nabla \times \bar{g}) = \bar{0} \ [N / m^3] \quad (42)$$

$\varepsilon_0 (\nabla . \bar{E}) = \rho_E$ Electric Charge Density [C/ m³]

in which: $\mu_0 (\nabla . \bar{H}) = \rho_M$ Magnetic Flux Density [Vs/ m³] or [Wb/ m³]

$\gamma_0 (\nabla . \bar{g}) = \rho_{Mass}$ Mass Density [kg/ m³]

Electric Energy Density: $w_E = \frac{1}{2} \varepsilon_0 E^2$

Magnetic Energy Density: $w_M = \frac{1}{2} \mu_0 H^2$

Gravitational Energy Density: $w_G = \frac{1}{2} \gamma_0 g^2$

$\bar{g} \triangleq$ acceleration (gravitational, linear- or orbital acceleration)

The black-colored terms in equation (42) are derived from well-established principles such as the Navier-Stokes Equation and Classical Electrodynamics. These terms are rooted in conventional scientific frameworks that have been widely accepted and utilized.

Conversely, the red-coloured terms in equation (42) originate from the New Theory, which introduces the concept of "Electro-Magnetic-Accelerated Field" interactions delineating the dynamic interplay between matter, notably the nuclear plasma, and energy represented by electric and magnetic fields. These red terms embody the innovative insights and novel theoretical perspectives brought forth by the New Theory, offering a fresh approach to understanding interactions between matter and energy within the system.

In equation (42) represents: $\overline{E_E}$ the external electric field intensity from the induced microwave radiation and the external induced Electric Fields in the DTT configuration with the three superconducting systems: the Toroidal (TF), the Poloidal (PF) Field and Central Solenoid (CS) Field, $\overline{E_P}$ the internal poloidal electric field intensity generated by the charged particles inside the plasma, $\overline{H_E}$ the external magnetic field intensity from the microwave radiation and the externally induced Magnetic Fields in the DTT configuration with the three superconducting systems: the Toroidal (TF), the Poloidal (PF) Field and Central Solenoid (CS) Field, $\overline{H_P}$ the internal (poloidal) magnetic field intensity generated inside the plasma by the spin of the ions, ζ represents the plasma dynamic viscosity, $\bar{v}$ the velocity, $\bar{g}$ the gravitational-, linear- or orbital- acceleration of the electric- and magnetic fields, p the pressure and $\bar{\bar{I}}$ the identity tensor in the Toroidal Tokamak Reactor.

7. Laminar- and Turbulent Plasma Flows

According Maxwell's equation, the magnetic part in Equation (42) can be reduced, only in "Laminar Plasma Flows" into:

$$\mu_0 \overline{H_E} \times (\nabla \times \overline{H_P}) = \mu_0 \overline{H_E} \times \overline{j_P} = \rho \overline{B_E} \times \bar{v} = -\rho \bar{v} \times \overline{B_E} = - \frac{1}{V_{Volume}} q \left(\bar{v} \times \overline{B_E} \right) \quad (43)$$

In which $\overline{\mathrm{j}_{P}}$ the electric current density of the laminar flow of electrically charged particle and “q” the electric charge of the particles.

According Gauss’s law, the electric part in Equation (42) can be reduced, only in “Laminar Plasma Flows” into:

$$- \varepsilon_0 \overline{E_E} (\nabla . \overline{E_P}) = - \overline{E_E} (\nabla . \overline{D_P}) = - \overline{E_E} \rho = - \frac{1}{V_{Volume}} q_P \overline{E_E} \tag{44}$$

Substituting (43) and (44) in (42) (only valid in laminar Plasma Flows) results in :

$$\begin{aligned} \bar{f} &= \rho \left(\frac{\partial \bar{v}}{\partial t} + \bar{v} \cdot \nabla \bar{v} \right) + \nabla p - \nabla \cdot \left(\zeta \left(\nabla \bar{v} + \left(\nabla \bar{v} \right)^T \right) - \frac{2}{3} \zeta \left(\nabla \cdot \bar{v} \right) \bar{\bar{I}} \right) \\ &- \frac{1}{V_{Volume}} q_P \left(\overline{E_E} + \bar{v} \times \overline{B_E} \right) + \frac{1}{c^2} \frac{\partial (\overline{E_E} \times \overline{H_E})}{\partial t} + \frac{1}{c^2} \frac{\partial (\overline{E_P} \times \overline{H_P})}{\partial t} + \varepsilon_0 \overline{E_E} \times (\nabla \times \overline{E_P}) \\ &- \mu_0 \overline{H_E} (\nabla . \overline{H_P}) - \bar{g} \left(\frac{1}{2 c^2} \left(\varepsilon E_E{}^2 + \mu H_E{}^2 \right) \right) - \gamma_0 \bar{g} (\nabla . \bar{g}) + \gamma_0 \bar{g} \times (\nabla \times \bar{g}) = \bar{0} \ [N / m^3] \end{aligned}$$

in which:

$$\begin{aligned} &\varepsilon_0 (\nabla . \bar{E}) = \rho_E \ \text{Electric Charge Density} \ [C/ m^3] \\ &\mu_0 (\nabla . \bar{H}) = \rho_M \ \text{Magnetic Flux Density} \ [Vs/ m^3] \text{ or } [Wb/ m^3] \\ &\gamma_0 (\nabla . \bar{g}) = \rho_{Mass} \ \text{Mass Density} \ [kg/ m^3] \\ &\text{Electric Energy Density:} \quad w_E = \frac{1}{2} \varepsilon_0 E^2 \\ &\text{Magnetic Energy Density:} \quad w_M = \frac{1}{2} \mu_0 H^2 \\ &\text{Gravitational Energy Density:} \quad w_G = \frac{1}{2} \gamma_0 g^2 \\ &\bar{g} \ \hat{=} \ \text{acceleration} \ (\text{gravitational, linear- or orbital acceleration}) \end{aligned} \tag{45}$$

The black coloured terms in equation (45) follow from the Navier Stokes Equation and Classical Electrodynamics. The red coloured terms in equation (45) follow from the New Theory describing “Electro-Magnetic-Accelerated Field” interactions between matter (nuclear plasma) and energy (electric- and magnetic fields).

In turbulent Plasma Flows only Equation (42) is valid.

8. Rotations of the Nuclear Plasma

A characteristic effect of the Nuclear Plasma, confined in a “Tokamak Reactor”, are the rotations of the Confined Nuclear Plasma in the Polar Direction and the Angular direction in Toroidal Coordinates [r, θ, ϕ, α. In which [θ] represents the angle in the polar direction and [ϕ]represents the angle of rotation in the azimuthal direction. The local radius has been represented by [r] and the radius of the Torus by [α] .

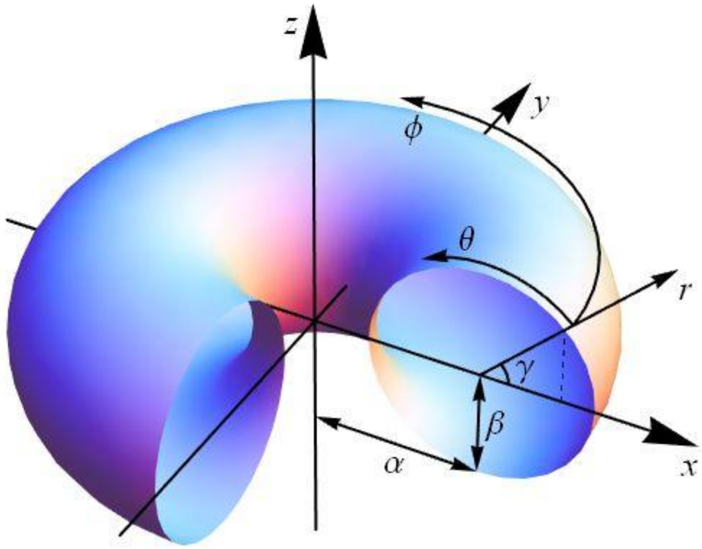

$$(r, \theta, \phi) = \left(\sqrt{\left(\sqrt{x^2 + y^2} - \alpha\right)^2 + z^2}, \left(\tan^{-1} \frac{z}{\sqrt{x^2 + y^2} - \alpha} \right) - \gamma, \tan^{-1} \frac{y}{x} \right)$$

$$(x, y, z) = ((\alpha + r\cos(\theta + \gamma))\cos\phi, (\alpha + r\cos(\theta + \gamma))\sin\phi, r\sin(\theta + \gamma))$$

Figure 13: Representation of Toroidal Coordinates

The force density, expressed in [N/ m³], causing the rotation of the Plasma in the Polar direction follows from equation (42) and has been represented in the color red and the force density, expressed in [N/ m³], causing rotation of the Plasma in the Azimuthal direction has been represented in the color green.

$$\begin{aligned} \bar{f} &= \rho \left(\frac{\partial \bar{v}}{\partial t} + \bar{v} \cdot \nabla \bar{v} \right) + \nabla p - \nabla \cdot \left(\zeta \left(\nabla \bar{v} + \left(\nabla \bar{v} \right)^T \right) - \frac{2}{3} \zeta \left(\nabla \cdot \bar{v} \right) \bar{\bar{I}} \right) \\ &- \varepsilon_0 \overline{E_E} (\nabla . \overline{E_P}) + \mu_0 \overline{H_E} \times (\nabla \times \overline{H_P}) + \frac{1}{c^2} \frac{\partial (\overline{E_E} \times \overline{H_E})}{\partial t} + \frac{1}{c^2} \frac{\partial (\overline{E_P} \times \overline{H_P})}{\partial t} + \varepsilon_0 \overline{E_E} \times (\nabla \times \overline{E_P}) \\ &- \mu_0 \overline{H_E} (\nabla . \overline{H_P}) - \bar{g} \left(\frac{1}{2 c^2} \left(\varepsilon E_E^2 + \mu H_E^2 \right) \right) - \gamma_0 \bar{g} (\nabla . \bar{g}) + \gamma_0 \bar{g} \times (\nabla \times \bar{g}) = \bar{0} \ [N/m^3] \end{aligned} \qquad [46]$$

in which:

$\varepsilon_0 (\nabla . \bar{E}) = \rho_E$ Electric Charge Density [C/ m³]

$\mu_0 (\nabla . \bar{H}) = \rho_M$ Magnetic Flux Density [Vs/ m³] or [Wb/ m³]

$\gamma_0 (\nabla . \bar{g}) = \rho_{Mass}$ Mass Density [kg/ m³]

Electric Energy Density: $w_E = \frac{1}{2} \varepsilon_0 E^2$

Magnetic Energy Density: $w_M = \frac{1}{2} \mu_0 H^2$

Gravitational Energy Density: $w_G = \frac{1}{2} \gamma_0 g^2$

$\bar{g} \triangleq$ acceleration (gravitational, linear- or orbital acceleration)

The force density, expressed in [N/ m³] causing the rotation of the Plasma in the Polar direction has been expressed by Equation [47]:

$$\overline{f_{\text{Polar Rotation}}} = -\varepsilon_0 \overline{E_{\text{External}}} (\nabla . \overline{E_P}) + \mu_0 \overline{H_{\text{Tokamak}}} \times (\nabla \times \overline{H_P}) \; [N/ m^3] \qquad [47]$$

In which the predominant terms, caused by the strong magnetic field inside the Tokamak, are colored magenta.

The force density, expressed in [N/ m³] causing the rotation of the Plasma in the Azimuthal Direction has been expressed by Equation [48]:

$$\overline{f_{\text{Azimuthal Rotation}}} = -\mu_0 \overline{H_{\text{Tokamak}}} (\nabla . \overline{H_P}) + \varepsilon_0 \overline{E_{\text{External}}} \times (\nabla \times \overline{E_P}) \; [N/ m^3] \qquad [48]$$

9. Equilibrium within Electromagnetically Confined Nuclear Plasma

From Equation (38) follows the 4-dimensional Electromagnetic-Dynamical Equilibrium Equation for Electromagnetically Confined Nuclear Plasma:

Energy-Time Domain

$$\nabla . \bar{S} + \frac{\partial w}{\partial t} = 0 \qquad [N / m^2 s]$$

3-Dimensional Space Domain

$$(49)$$

$$\bar{f} = \rho \left(\frac{\partial \bar{v}}{\partial t} + \bar{v} \cdot \nabla \bar{v} \right) + \nabla p - \nabla \cdot \left(\zeta \left(\nabla \bar{v} + \left(\nabla \bar{v} \right)^T \right) - \frac{2}{3} \zeta \left(\nabla \cdot \bar{v} \right) \bar{\bar{I}} \right)$$
$$- \varepsilon_0 \overline{E_E} (\nabla . \overline{E_P}) + \mu_0 \overline{H_E} \times (\nabla \times \overline{H_P}) + \frac{1}{c^2} \frac{\partial (\overline{E_E} \times \overline{H_E})}{\partial t} + \frac{1}{c^2} \frac{\partial (\overline{E_P} \times \overline{H_P})}{\partial t} + \varepsilon_0 \overline{E_E} \times (\nabla \times \overline{E_P})$$
$$- \mu_0 \overline{H_E} (\nabla . \overline{H_P}) - \bar{g} \left(\frac{1}{2 c^2} \left(\varepsilon E_E^{\,2} + \mu H_E^{\,2} \right) \right) - \gamma_0 \bar{g} (\nabla . \bar{g}) + \gamma_0 \bar{g} \times (\nabla \times \bar{g}) = \bar{0} \; [N / m^3]$$

Which can be written a:

Energy-Time Domain

$$\nabla . (\overline{E_P} \times \overline{H_P}) + \frac{1}{2} \frac{\partial \left(\varepsilon E_E^{\,2} + \mu H_E^{\,2} \right)}{\partial t} = 0 \qquad [N / m^2 s]$$

3-Dimensional Space Domain

$$\bar{f} = \rho \left(\frac{\partial \bar{v}}{\partial t} + \bar{v} \cdot \nabla \bar{v} \right) + \nabla p - \nabla \cdot \left(\zeta \left(\nabla \bar{v} + \left(\nabla \bar{v} \right)^T \right) - \frac{2}{3} \zeta \left(\nabla \cdot \bar{v} \right) \bar{\bar{I}} \right) \qquad (50)$$
$$- \varepsilon_0 \overline{E_E} (\nabla . \overline{E_P}) + \mu_0 \overline{H_E} \times (\nabla \times \overline{H_P}) + \frac{1}{c^2} \frac{\partial (\overline{E_E} \times \overline{H_E})}{\partial t} + \frac{1}{c^2} \frac{\partial (\overline{E_P} \times \overline{H_P})}{\partial t} + \varepsilon_0 \overline{E_E} \times (\nabla \times \overline{E_P})$$
$$- \mu_0 \overline{H_E} (\nabla . \overline{H_P}) - \bar{g} \left(\frac{1}{2 c^2} \left(\varepsilon E_E^{\,2} + \mu H_E^{\,2} \right) \right) - \gamma_0 \bar{g} (\nabla . \bar{g}) + \gamma_0 \bar{g} \times (\nabla \times \bar{g}) = \bar{0} \; [N / m^3]$$

10. Conclusion

The interaction between Gravity and Light is effectively described in General Relativity through a 4-dimensional curvature encompassing Space and Time due to the presence of a gravitational field. Light follows a trajectory dictated by this curved 4-dimensional Space-Time geometry.

Contrasting with General Relativity, the new theory introduces a novel concept where mass and inertia within light, represented by photons, exhibit a bi-directional separation. Inertia specifically manifests along the beam's propagation, impacting the speed of light, while mass is oriented perpendicularly, influencing light deflection by gravitational fields [39-45]. BLACK HOLES, representing Gravitational-Electromagnetic Confinements, serve as fundamental solutions derived from the relativistic quantum mechanical Dirac equation, showcasing significant "Gravitational Intensity Shift" and "Gravitational RedShift" phenomena.

The new theory delves into gravitational fields around BLACK HOLES, investigating the phenomenon of "CURL" within these regions, as well as exploring Gravitational Lensing effects. Gravitational-Electromagnetic Confinements at subatomic dimensions characterize physical reality, forming solutions of the Relativistic Quantum Mechanical Dirac Equation, presenting discrete energy levels within spherical confines.

Validating this new theory against General Relativity demands precise experiments measuring Gravity-Light interactions. The distinction in Gravitational RedShift predictions between General Relativity and the New Theory, though minute (smaller than 10-16), necessitates improved observation equipment for validation. Dark Matter's existence, inferred from Gravitational RedShift and Gravitational Intensity Shift effects, elucidates cosmic invisibility implicating billions of light-emitting galaxies beyond the "Gravitational Shielding" radius.

In the domain of nuclear fusion, a new theoretical approach accommodating "mechanical-electromagnetic" interactions in compressible nuclear plasmas espouses stability requirements. Equations (42) and specifically laminar Plasma Flows (45) signify the 3-dimensional equilibrium between dynamic- and electromagnetic force densities crucial for ensuring the fundamental stability essential for successful nuclear fusion endeavours.

Data Availability

All Data and Calculations have been published at:

https://quantumlight.science/

References

1. Wheeler., Archibald, J. (1955). GEONs, Physical Review Journals Archive, 97, 511, Issue 2, pages 511-526, Published 15 January 1955, Publisher: American Physical Scociety.
2. Herrmann, S., Finke, F., Lülf, M., Kichakova, O., Puetzfeld, D., Knickmann, D., ... & Lämmerzahl, C. (2018). Test of the gravitational redshift with Galileo satellites in an eccentric orbit. *Physical review letters, 121*(23), 231102.
3. Vegt, W. (1995). A continuous model of matter based on AEONs.
4. Wim, V. Mathematical Solutions for the Propagation of Light in Quantum Light Theory. Calculations in Mathematica, 13.
5. Wim, V. (2023). Gravitational RedShift between two atomic clocks. Calculation, 2, 16.
6. Wim, V. (2022). Propagation of light within a gravitational field in quantum light theory. Calculation in Mathematica, 13.
7. Beach, R. J. (2014). A Classical Field Theory of Gravity and Electromagnetism. *Journal of Modern Physics, 5*(10), 928-939.
8. Maxwell, J. C. (1865). VIII. A dynamical theory of the electromagnetic field. *Philosophical transactions of the Royal Society of London,* (155), 459-512.
9. Einstein, A. (1911). On the Influence of Gravitation on the Propagation of Light. *Annalen der Physik, 35*(898-908), 906.
10. Goray, M., & Annavarapu, R. N. (2020). Rest mass of photon on the surface of matter. *Results in Physics, 16,* 102866.
11. Genova, A., Mazarico, E., Goossens, S., Lemoine, F. G., Neumann, G. A., Smith, D. E., & Zuber, M. T. (2018). Solar system expansion and strong equivalence principle as seen by the NASA MESSENGER mission. *Nature communications, 9*(1), 289.
12. Williamson, J. G. (2019). A new linear theory of light and matter. In *Journal of Physics: Conference Series* (Vol. 1251, No. 1, p. 012050). IOP Publishing.
13. Wim, V. (2023). Black holes with discrete spherical energy levels. Calculation, 4, 21.
14. Wim, V. (2023). Time and Radius dependent GEONs with discrete Energy Levels. Calculation 5; 16 March.
15. Wim, V. (2023). Time and Angular Regions dependent GEONs with discrete energy levels.
16. Wim, V. (2023). Time and Azimuthal Regions dependent GEONs with discrete energy levels, Calculation 7; 15 May.
17. Wim, V. (2023). Time, Polar Angular and Azimuthal Angular Regions dependent GEONs with discrete energy levels.
18. Sciama, D. W. (1964). The physical structure of general relativity. *Reviews of Modern Physics, 36*(1), 463.
19. Del Rio, A., Navarro-Salas, J., & Torrenti, F. (2014). Renormalized stress-energy tensor for spin-1/2 fields in expanding universes. *Physical Review D, 90*(8), 084017.
20. Pellis, S. (2022). Unity formulas for the coupling constants and the dimensionless physical constants. *Journal of High Energy Physics, Gravitation and Cosmology, 9*(1), 245-294.

21. Bloch, Y., & Foo, J. (2023). How the result of a measurement of a photon's mass can turn out to be 100. *arXiv preprint arXiv:2305.00891*.
22. García, A. A., Bondarenko, K., Ploeckinger, S., Pradler, J., & Sokolenko, A. (2020). Effective photon mass and (dark) photon conversion in the inhomogeneous Universe. *Journal of Cosmology and Astroparticle Physics, 2020*(10), 011.
23. Gabovich, A. M., & Gabovich, N. A. (2007). How to explain the non-zero mass of electromagnetic radiation consisting of zero-mass photons. *European Journal of Physics, 28*(4), 649.
24. Tu, L. C., Luo, J., & Gillies, G. T. (2004). The mass of the photon. *Reports on Progress in Physics, 68*(1), 77.
25. Doyon, B. (2013). Conformal loop ensembles and the stress–energy tensor. *Letters in Mathematical Physics, 103*(3), 233-284.
26. Hack, T. P., & Moretti, V. (2012). On the stress–energy tensor of quantum fields in curved spacetimes—comparison of different regularization schemes and symmetry of the Hadamard/Seeley–DeWitt coefficients. *Journal of Physics A: Mathematical and Theoretical, 45*(37), 374019.
27. Levi, A. (2017). Renormalized stress-energy tensor for stationary black holes. *Physical Review D, 95*(2), 025007.
28. Gobbi, J. (2018). Luminiferous Æther: General Science Journal.
29. Ye, X. H., & Lin, Q. (2008). Gravitational lensing analysed by the graded refractive index of a vacuum. *Journal of Optics A: Pure and Applied Optics, 10*(7), 075001.
30. Vegt, W. (2023). The Origin of Gravity in “Quantum Light Theory”.
31. Delva, P., Puchades, N., Schönemann, E., Dilssner, F., Courde, C., Bertone, S., & Wolf, P. (2018). Gravitational redshift test using eccentric Galileo satellites. *Physical review letters, 121*(23), 231101.
32. Oppenheim, J. (2023). A postquantum theory of classical gravity?. *Physical Review X, 13*(4), 041040.
33. Vegt, W. (2022). The Origin of Gravity, A second order Lorentz Transformation for" Accelerated Electromagnetic Fields", Generating a Gravitational Field and the property of Mass.
34. Vegt, W. (2021). The 4-dimensional dirac equation in relativistic field theory. *European Journal of Applied Sciences, 9*(1), 35-93.
35. Vegt, W. (2023). A Perfect Equilibrium inside a Black Hole; Wolfram Community.
36. Einstein, A. (1953). Elementary considerations for the interpretation of the foundations of quantum mechanics.
37. Lobos, N. J. L. S., & Pantig, R. C. (2022). Generalized extended uncertainty principle black holes: shadow and lensing in the macro- and microscopic realms. *Physics, 4*(4), 1318-1330.
38. Weng, Z. (2008). Influence of velocity curl on conservation laws.
39. Vadasz, P. (2016). Rendering the Navier–Stokes Equations for a Compressible Fluid into the Schrödinger Equation for Quantum Mechanics. *Fluids, 1*(2), 18.
40. Kwon, Y. S. (2018). Asymptotic limit for rotational quantum compressible Navier–Stokes equations with multiple scales. *Journal of Mathematical Analysis and Applications, 464*(2), 1408-1424.
41. Shimizu, S., & Tsuritani, H. (2021). On a Navier–Stokes–Ohm problem from plasma physics in multi connected domains. *Partial Differential Equations and Applications, 2*(6), 75.
42. Cambier, J. L., Micheletti, D. A., & Bushnell, D. M. (2000). Theoretical analysis of the electron spiral toroid concept (No. NAS 1.26: 210654.
43. Soraya Field Fiorio, Isaac Newton: Magician.
44. Sethian, J. D., Friedman, M., Lehmberg, R. H., Myers, M., Obenschain, S. P., Giuliani, J., & Lucas, G. (2003). Fusion energy with lasers, direct drive targets, and dry wall chambers. *Nuclear Fusion, 43*(12), 1693.
45. Degrave, J., Felici, F., Buchli, J., Neunert, M., Tracey, B., Carpanese, F., & Riedmiller, M. (2022). Magnetic control of tokamak plasmas through deep reinforcement learning. *Nature, 602*(7897), 414-419.